A&A 382, 804–820 (2002)
DOI: 10.1051/0004-6361:20011708

Astronomy & Astrophysics

The new emerging model for the structure of cooling cores in clusters of galaxies

H. Böhringer[1], K. Matsushita[1], E. Churazov[2], Y. Ikebe[1], and Y. Chen[1]

[1] Max-Planck-Institut für Extraterrestrische Physik, 85748 Garching, Germany
[2] Max-Planck-Institut für Astrophysik, 85748 Garching, Germany

Received 22 August 2001 / Accepted 7 November 2001

Abstract. New X-ray observations with XMM-Newton show a lack of spectral evidence for large amounts of cooling and condensing gas in the centers of galaxy clusters believed to harbour strong cooling flows. This paper re-explores the cooling flow scenario in the light of the new observations. We explore the diagnostics of the temperature structure of cooling cores with XMM-spectroscopy, tests for intracluster X-ray absorption towards central AGN, the effect of metal abundance inhomogeneities, and the implications of high resolution images in the centers of clusters. We find no evidence of intrinsic absorption in the center of the cooling flows of M 87 and the Perseus cluster. We further consider the effect of cluster rotation in cooling flow regions in the frame of cosmic structure evolution models. Also, the heating of the core regions of clusters by jets from a central AGN is reconsidered. We find that the power of the AGN jets as estimated by their interaction effects with the intracluster medium in several examples is more then sufficient to heat the cooling flows and to reduce the mass deposition rates. We explore in more detail which requirements such a heating model has to fulfill to be consistent with all observations, point out the way such a model could be constructed, and argue that such model building seems to be successful. In summary, it is argued that most observational evidence points towards much lower mass deposition rates than previously inferred in the central region of clusters thought to contain strong cooling flows.

Key words. galaxies: clusters: general – X-rays: galaxies: clusters

1. Introduction

With first detailed X-ray observations using the *UHURU* and *Copernicus* satellites and the first rocket borne X-ray telescopes it was discovered that the X-ray emitting, hot gas in galaxy clusters reaches high enough densities in the cluster centers that the cooling time of the gas falls below the Hubble time. The consequences of these observations have first been explored in early papers by Silk (1976), Fabian & Nulsen (1977), Cowie & Binney (1977), and Mathews & Bregman (1978). In the absence of a suitable fine-tuned heating source, the cooling and condensation of the gas in the central regions is a straight-forward consequence of the energy equation of the hot gas. From this analysis the cooling flow scenario emerged (e.g. Fabian et al. 1984; Fabian 1994). This scenario obtained very early strong support from spectroscopic observations with the *Einstein observatory Solid State Spectrometer* and *Focal Plane Cristal Spectrometer* instruments. It was found that the spectra imply an emission measure distribution of the gas as a function of temperature showing low temperature phases in addition to the hotter temperature gas and a distribution function in temperature consistent with steady state cooling (Canizares et al. 1979, 1982; Mushotzky & Szymkowiak 1988). This spectroscopic diagnostic remained one of the strongest bases for the foundation of the cooling flow picture until now, where *XMM-Newton* and *Chandra* are finally providing high resolution X-ray spectra superseeding those obtained with the *Einstein* instruments.

Detailed analysis of surface brightness profiles of X-ray images of clusters obtained with the *Einstein* observatory and further theoretical work led to the detailed, self-consistent scenario of inhomogeneous, comoving cooling flows (Nulsen 1986; Thomas et al. 1987). The main assumptions on which this model is based and some important implications are: (i) Each radial zone in the cooling flow region comprises different plasma phases covering a wide range of temperatures. The consequence of this temperature distribution is that gas will cool to low temperature and condense over a wide range of radii. This is in contrast to a homogeneous cooling flow where the hot plasma would only condense and be deposited in the center, implying a very peaked surface brightness profile which is not observed (e.g. Fabian 1994). (ii) The gas comprising different temperature phases features an inflow in which all phases move with the same flow speed, forming a comoving cooling flow. (iii) There is no energy exchange

Send offprint requests to: H. Böhringer,
e-mail: hxb@mpe.mpg.de

between the different phases, between material at different radii, and no heating. This means in particular that heat conduction has to be suppressed to a negligible value (e.g. Fabian et al. 1994). When all these premises are taken together, the inhomogeneity of the cooling flow is a direct consequence of the observed X-ray surface brightness profile as observed for those clusters of galaxies which feature a low central cooling time (Thomas et al. 1987).

Further X-ray observations brought relatively little new support for this detailed scenario in the last about 15 years. *ROSAT* observations showed that the central regions in cooling flow clusters have a lower temperature than the outer regions (e.g. Schwarz et al. 1992). Spectroscopic studies with *ASCA* provided evidence that there is at least more than one temperature phase present in cluster centers (e.g. Fabian et al. 1994; Ikebe et al. 1997, 1999; Makishima et al. 2001). But these spectroscopic data obtained with *ASCA* are not sufficient to allow a detailed test of the cooling flow model by the reproduction of the predicted emission measure distribution as a function of temperature as predicted for the inhomogeneous cooling flow model (e.g. Johnstone et al. 1992). One further interesting piece of observational evidence was the spectral signature of excess absorption in addition to the absorption expected for the interstellar medium of our galaxy (e.g. White et al. 1991). This excess absorption originates most probably in the galaxy cluster centers. It was taken as further support for the cooling flow model since it provides evidence that gas has cooled from the cooling flow to low temperature (e.g. Fabian 1994; Allen et al. 2001).

It remained a puzzle, however, that for the regions with cooling flows with estimated mass deposition rates up to several hundred or thousand solar masses per year, little evidence for such massive cooling of gas could be found at other wavelengths (e.g. Fabian 1994). This is a major reason why the cooling flow model is not accepted unanimously among astronomers. Evidence for warm gas (diffuse emission line systems), cool gas, and even star formation was well detected at lower levels (e.g. Heckman et al. 1989; Fabian 1994). In a recent review of indications of star formation in cooling flows McNamara (1997) showed that the inferred star formation rates are typically only in the range of 1 to 10% of the model predicted mass deposition rates and range from 1 to $<100\ M_\odot\ \mathrm{yr}^{-1}$ (e.g. McNamara & O'Connell 1989, 1993; Crawford & Fabian 1992; Allen 1995; Cardiel et al. 1998; Crawford et al. 1999). Very recently interesting observations of molecular emission lines from CO and indications of warm dust have lead to the implications of a larger reservoir of cold gas in cooling flows (Wilman et al. 2000; Edge 2001; Edge et al. 1999). These observations provide stronger support to the idea that mass deposition may happen in the more massive cooling flows, but they do not necessarily confirm the very high mass deposition rates inferred for these clusters from X-ray imaging data.

Therefore there was little means from observational data to prove or disprove the existence of inhomogeneous cooling flows with massive mass deposition rates and one was awaiting better opportunities for more detailed X-ray spectroscopic observations to further test the cooling flow picture. The Japanese *ASTRO E* would have been a prime instrument for such studies, but very unfortunately it was lost in a launch accident. Now the first analysis of high resolution X-ray spectra and imaging spectroscopy obtained with *XMM-Newton* has supplied us with the first surprises which could lead to a breakthrough in this long-standing debate. The first surprise is that the spectra show no signatures of cooler phases of the cooling flow gas below an intermediate temperature, which constitutes a problem for the interpretation of the results in the conventional cooling flow picture (e.g. Peterson et al. 2001; Tamura et al. 2001). Another result is that the spectroscopic data are better explained with local isothermality in the cooling flow region (e.g. Matsushita et al. 2001; Molendi & Pizzolato 2001), that is also in conflict with the inhomogeneous cooling flow model.

In this paper we discuss these new spectroscopic results and their implications, review some further unsolved issues concerning cooling flows, and point out the way to a new model for this phenomenon. Section 2 is concerned with the spectroscopic evidence of the absence of low temperature phases and the local isothermality in cooling flow regions. We take examples for the results mainly from the best observed case, the X-ray halo of M 87 in the X-ray emission center of the Virgo cluster. In Sects. 3 and 4 we discuss the evidence for internal absorption in cooling flows in the light of new results using the AGN in the center of clusters as independent probes. Section 5 is devoted to a discussion of surface brightness inhomogeneities observed in cooling flow regions as possible sites of mass deposition. In Sect. 6 we review the problem of cooling flows in rotating clusters with respect to the expectation values for angular momentum in clusters in the frame of cosmological models. In Sect. 7 we discuss the requirements for a suitable heating model and explore if such a heating model can be devised on the basis of the energy input from AGN in the cluster centers. In Sect. 8 we address the implications of the strong observed magnetic fields in cooling flow regions and Sect. 9 provides our conclusions. Since we argue for strongly reduced mass condensation rates which are more localized in the very central regions, we will term the cooling flow regions "cluster cooling cores" in the following.

For the physical parameters of galaxy clusters that scale with distance we use a Hubble constant of $H_0 = 50\ \mathrm{km\,s^{-1}\ Mpc^{-1}}$.

2. Spectroscopic evidence for the absence of low temperature phases and local isothermality in cooling flow regions

Recent results from XMM-Newton (Jansen et al. 2001) observations have provided unpreceded detailed spectroscopic diagnostics of the central regions of clusters providing new insights into the structure of cooling core regions. One set of observations is obtained with the

XMM Reflection Grating Spectrometer (RGS, den Herder et al. 2001). They show for several cooling core regions spectral signatures of different temperature phases ranging approximately from the hot virial temperature of the cluster to a lower limiting temperature, $T_{\rm low}$, which is still significantly above the "drop out" temperature where the gas would cease to emit significant X-ray radiation. That is, the clearly observable spectroscopic features of the lower temperature gas expected for a cooling flow model are not observed. In the case of the massive, cooling flow cluster A1835 with a bulk temperature of about 8.3 keV no lines or features for temperature phases below 2.7 keV are found (Peterson et al. 2001). Similar results have been derived for the cluster A1795 (Tamura et al. 2001).

In the standard cooling flow model the spectral luminosity from the different temperature phases is fixed by the mass flow rate of the cooling flow in such a way that the emission measure for each temperature interval, $[T, T + {\rm d}T]$, from the hottest temperatures to the "drop out" temperature, is proportional to the mass flow rate, $\dot{M}$, and given by (e.g. Johnstone et al. 1992)

$$L_\nu(T)\ {\rm d}T \ = \ \frac{\Lambda_\nu(T)}{\Lambda_{\rm cool}(T)}\ \frac{5k_{\rm B}}{2\mu m_{\rm p}}\ \dot{M}\ {\rm d}T, \qquad (1)$$

where $\Lambda_\nu(T)$ and $\Lambda_{\rm cool}(T)$ are the emissivity at frequency ν and the bolometric emissivity, respectively, and $\mu m_{\rm p}$ is the mean particle mass in the hot plasma. The total spectrum is then given by the integral

$$L_\nu \ = \frac{5k_{\rm B}}{2\mu m_{\rm p}}\ \dot{M}\ \int_0^{T_{\rm max}} \frac{\Lambda_\nu(T)}{\Lambda_{\rm cool}(T)}{\rm d}T. \qquad (2)$$

Therefore, if the mass deposition rate determined from the surface brightness distribution is known, the spectral signature of each temperature phase of the cooling flow is fixed and the total spectrum can be predicted. That the expected low temperature signatures are not observed is therefore in clear conflict with the standard cooling flow model.

These results coming from the *XMM RGS* data are confirmed by *XMM-Newton* observations with the energy sensitive imaging devices, EPN (Strüder et al. 2001) and EMOS (Turner et al. 2001). Even though the spectral resolution is less for these instruments than for the RGS they can very well be used to detect temperature sensitive spectral features with high accuracy due to the good photon statistics. They have the additional advantage of providing spectral information across the entire cooling core region. First the spectral fitting of the X-ray emission in the cooling flow clusters M 87, A1795, A496, and A1835 showed that single temperature models provided a better representation of the data than cooling flow models (Böhringer et al. 2001; Molendi & Pizzolato 2001), also implying the lack of low temperature components. In a recent, very detailed analysis of the temperature structure of the closest and best studied cooling flow in M 87, Matsushita et al. (2001) have shown that the temperature structure is well described locally by a single temperature over most of the cooling core region. In particular the spectral features originating from gas below a temperature of about 0.8–1 keV, as predicted by the standard cooling flow model through the above formula, are not detected. The approximate local isothermality of the gas is shown very well by the overall consistency of the fitting of complete spectra as well as by the study of special features as e.g. the spectral feature of the blend of Fe L-shell lines and the ratio of the hydrogen like to helium like emission lines in Si and S. An exception is the central region ($r \leq 1$ arcmin, $\sim$5 kpc) which is also disturbed by the interaction of the jet and the inner radio lobes, where a narrow range of temperatures (well within 0.8–2 keV) is indicated in the spectra. One should note that the results derived by Matsushita et al. (2001) have in contrast to most other work been obtained from deprojected spectra in concentric rings, which feature within the validity of the assumption of approximate spherical symmetry the spectral emission of three-dimensional volume elements. In fact the practically perfect fit with isothermal spectra was only achieved after deprojection. The effort of deprojecting the spectra is of course especially rewarding in the case of M 87 due to the high spatial resolution (8 arcsec correspond to about 0.7 kpc at M 87) and the excellent photon statistics (for e.g. the PN more than 12 million photons were received in the useful observing period).

It was also discovered in the analysis of the M 87 X-ray spectra that the emission from the innermost region ($r \leq 1$ arcmin) is most probably effected by resonant line scattering in some of the most prominent emission lines, an effect that severely disturbs the measurement of element abundances (Böhringer et al. 2001). This could in principle be made responsible for the lack of some of the spectral lines indicative of low temperature material in the cooling flow as observed with the RGS instrument. In the detailed analysis of the EPN and EMOS spectra this problem could be avoided, however, by integrating over a large enough radial region that the net effect of resonant line scattering is negligible (almost all the scattered light will be re-emitted close to the center), and therefore it could be established that the lack of low temperature emission lines is not an artefact due to resonant line scattering (Matsushita et al. 2001).

2.1. The Fe-L-shell lines as ICM thermometer

Among the spectroscopic signatures which are sensitive to the temperature of the hot plasma in the temperature range relevant to cooling flows, the complex of iron L-shell lines is most important. Therefore we will illustrate its use as a sensitive thermometer of the intracluster temperature structure in more detail. It has e.g. also been used in the *XMM-Newton* study of the temperature structure of the X-ray surface brightness excess features at the location of the inner radio lobes of M 87 by Belsole et al. (2001). Figure 1 shows simulated X-ray spectra as predicted for the XMM EPN instrument in the spectral region around the Fe L-shell lines for a single-temperature plasma

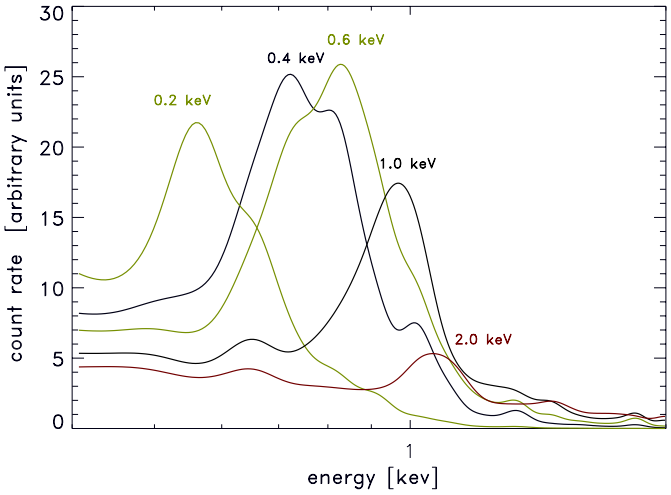

Fig. 1. The Fe L-line complex in X-ray spectra as a function of the plasma temperature for a metallicity value of 0.7 solar. The simulations show the appearance of the spectra as seen with the XMM EPN. The emission measure was kept fixed when the temperature was varied.

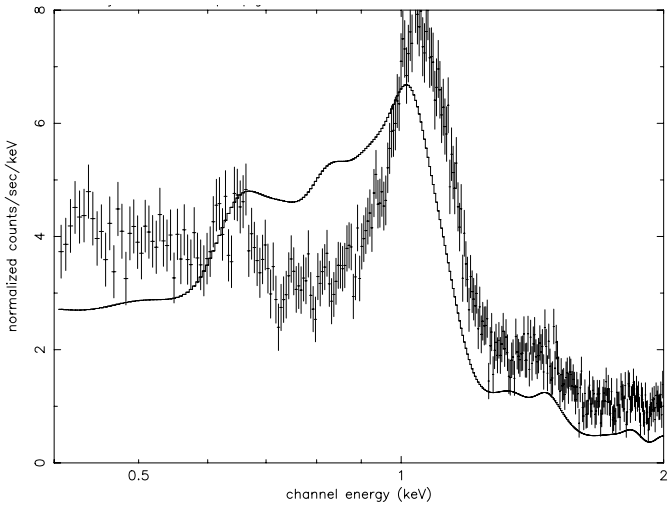

Fig. 2. *XMM EPN*-spectrum of the central region of the M 87 X-ray halo in the radial range $R = 1{-}2$ arcmin. The spectrum has been fitted with a cooling flow model with a best fitting mass deposition rate of 0.96 $M_\odot$ yr^{-1}, a fixed absorption column density of 1.8×10^{20} cm^{-2}, the galactic value, and a parameter for $T_{\rm low}$ of 0.01 keV.

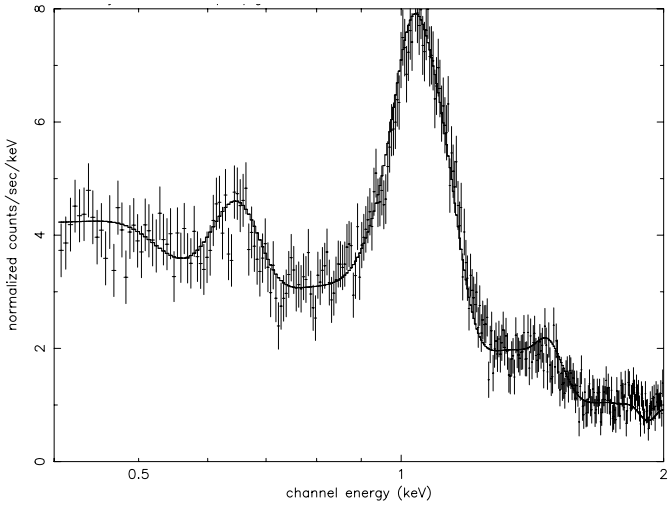

Fig. 3. *XMM EPN*-spectrum of the central region of the M 87 X-ray halo in the radial range $R = 1{-}2$ arcmin fitted by a cooling flow spectrum artificially constraint to emission from the narrow temperature interval 1.44–2.0 keV yielding a mass deposition rate of 2.4 $M_\odot$ yr^{-1}. The parameter $T_{\rm low}$ was treated as a free fitting parameter.

at various temperatures from 0.4 to 2.0 keV and 0.7 solar metallicity as measured for the iron abundance in the central region of the M 87 halo. There is a very obvious shift in the location of the peak of the blend of iron L-shell lines. This energy change is caused by the fact that with decreasing temperature the degree of ionization of the Fe ions also decreases. The resulting effect is an increased screening of the charge of the nucleus and a decreased binding energy of the L-shell electrons which is reflected in a decreasing transition energy for L-shell lines. This effect turns out to provide an excellent thermometer in particular for the energy range shown.

For a cooling flow with a broad range of temperatures one expects a composite of several of the relatively narrow line blend features, resulting in a quite broad peak for the blend of iron L-shell lines. Figure 2 shows for example the deprojected spectrum of the M 87 halo plasma for the radial range 1–2 arcmin (outside the excess emission region at the inner radio lobes) and a fit of a cooling flow model with a mass deposition rate slightly less than 1 $M_\odot$ yr^{-1}, as approximately expected for this radial range of the cooling core from the analysis of the surface brightness profile (e.g. Stewart et al. 1984; Allen et al. 2001; Matsushita et al. 2001). We have selected this radial region to best demonstrate the diagnostics of the cooling core, since it is far enough away from the central nucleus and jet not to be contaminated by these non-thermal X-ray sources, yet is still very centrally located in the cooling core, and provides a good photon statistics due to the high surface brightness.

It is evident that the peak in the cooling flow model is much broader than the observed spectral feature. For comparison Fig. 3 shows the same spectrum fitted by a cooling flow model where a temperature of 2 keV was chosen for the maximum temperature and a suitable lower temperature cut-off was determined by the fit. As expected from the observed narrow peak shape, only a narrow temperature range is allowed by the fit with a lower temperature cut-off at 1.44 keV. This is only meant as an example, and the value for $T_{\rm low}$ depends here slightly on the value chosen for the fixed value for $T_{\rm max}$. For a detailed discussion of the best constraints on isothermal model fits to the complete spectra see Matsushita et al. (2001). The discrepancy between the predictions of the cooling flow model and the observations is indeed striking and even more obvious than the discrepancies found for the RGS spectra of the more massive and hotter cooling flow clusters mentioned above. In the next two subsections we therefore explore

possibilities to reconcile the observations with the cooling flow expectations.

2.2. Inhomogeneous metal abundances in the ICM

One of the effects that could possibly rectify the standard cooling flow scenario with the observed spectral properties of cooling flow regions, as suggested by Fabian et al. (2001a), is a very inhomogeneous distribution of the metal abundances in the cluster ICM. From the above discussion it is obvious that the spectral diagnostics are essentially based on the observation of spectral lines from metal elements. Therefore without a significant metal abundance the signatures searched for are absent. The model proposed by Fabian et al. recognises that the intensity of the metal lines in the spectra is not simply proportional to the abundance. Since the total amount of radiation power that can be emitted by the cooling gas is limited by the gas's heat capacity, there is a saturation effect in the line intensities, if the fraction of the emission power contributed by the lines is large. This situation is most severe at low temperatures. The application of this effect to cooling flow models where the total emission power for each temperature phase is fixed by the mass deposition rate through Eq. (1) is most interesting: the line intensity reduction due to an inhomogeneous metal distribution is most effective for the low temperature phases, an effect that could in principle be responsible for the non-detection of the low-temperature lines.

We can cast this argument into mathematical form to explore in more detail how the apparent abundance distribution is affected by an inhomogeneous metallicity of the intracluster plasma. In the following calculation we investigate in a simplified but very illustrative model how the apparent metallicity changes if we start with a mean metallicity, z, which is distributed unevenly in two plasma phases with the same temperature. We make the further simplifying assumption that phase 1 is completely devoid of metals and phase 2 is enriched. We calculate the apparent metallicity that is derived if the resulting combined spectrum is analysed under the assumption of a chemically homogeneous plasma. The apparent metallicity is proportional to the observed intensity ratio of the lines to the continuum. The change in the apparent metallicity is thus equivalent to the suppression factor of the line signature of the cooling flow at low temperature. This two-phase model is an approximate and simple representation of the scenario described by Fabian et al. (2001a) in which the minor ICM component is heavily enriched by recent SN Ia and stellar wind contributions while the bulk of the gas has relatively low metallicity.

For the model we define the following important parameters: z is the mean metallicity in solar units as defined above, f is the mass fraction of the enriched plasma phase, $z_2 = z \cdot f^{-1}$ is the metallicity of the enriched phase, and $< z_{\rm obs} >$ is the mean apparent ("observed") metallicity. We further define the parameter $\mathcal{F}$ as the fraction of the emitted flux in metal lines as compared to the total emission, and $\mathcal{F}_1$ as this fraction for the case of solar metallicity ($z = 1$) of a homogeneous medium. $\mathcal{F}_2$ then designates the line intensity fraction for the enriched second phase of the inhomogeneous ICM model.

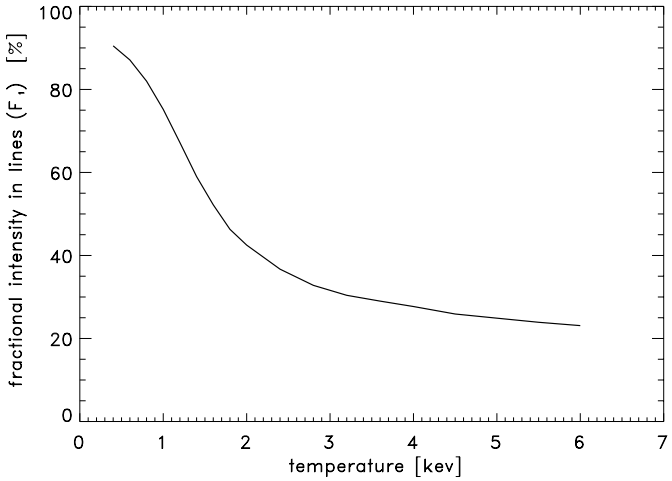

Fig. 4. Fraction of radiative emission power that is contributed by the metal ions in the plasma, $\mathcal{F}_1$, as a function of temperature for a solar abundance plasma (with abundances from Anders & Grevesse 1989).

The parameter $\mathcal{F}_1$ is an important indicator that divides the metallicity range in which $\mathcal{F}$ is proportional to z and for which $\mathcal{F}$ is in the saturation regime. The values of $\mathcal{F}_1$ as a function of plasma temperature in the temperature range relevant for the present discussion are given in Fig. 4. The formulae used to calculate $\mathcal{F}$ as well as the basics of the following calculations are derived in detail in the Appendix. We note in Fig. 4 that $\mathcal{F}_1$ is increasing with decreasing temperature, the saturation effects leading finally to a suppression of the apparent, observed metallicity will therefore be most effective at low temperatures, as suggested by Fabian et al. (2001a).

The apparent, observed metallicity can then be calculated by means of the following formula:

$$< z_{\rm obs} >= \frac{z\ (1 - \mathcal{F}_1)}{1\ +\ z\mathcal{F}_1\ (zf^{-1} - z - 1)}. \qquad (3)$$

Figure 5 shows the resulting apparent metallicity as a function of the mass fraction (equal to the emission measure fraction) of the enriched gas. Here the mean metallicity, z, has been taken to be 0.7 of the solar value as measured for iron in the central region of the M 87 X-ray plasma halo. We note that the suppression of the metal lines is very dramatic for low temperatures. Therefore this effect should in general be taken very seriously and for each case of a metallicity determination at these low temperatures we have to check carefully if a homogeneous chemical distribution can be assumed or if corrections for an inhomogeneous distribution might apply.

Inspecting Fig. 5 we note two interesting effects. Firstly, if we want to suppress the line emission e.g. for the temperature phase with $T = 0.4$ keV by an order of

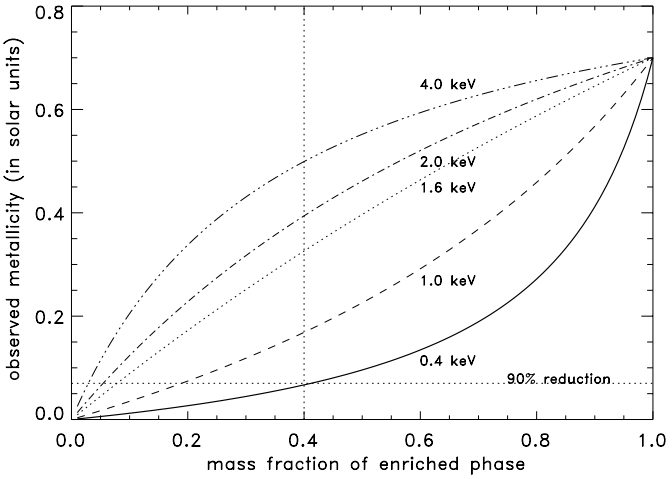

Fig. 5. Apparent deduced metallicity from the spectrum emitted from a chemically inhomogeneous two-component plasma as a function of temperature when a single-phase plasma is assumed in the analysis. The mean metallicity in the model is 0.7 solar. Results for different plasma temperatures are given in the plot. For further explanations see the text.

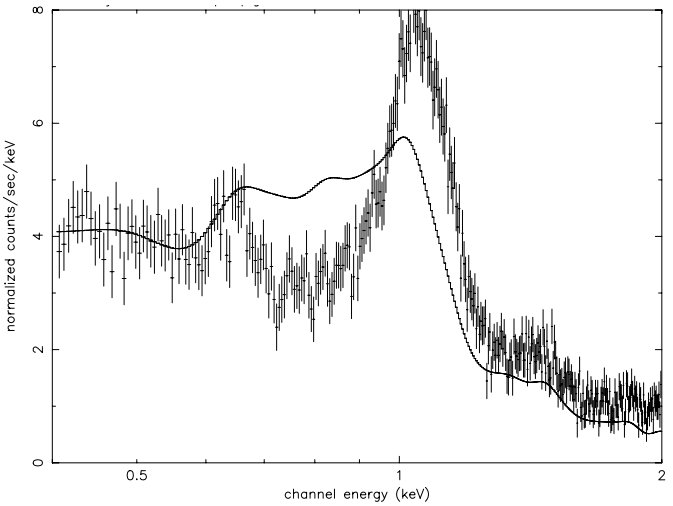

Fig. 6. *XMM*-spectrum of the 1–2 arcmin region in the M 87 halo fitted by a model with two cooling flow phases, one with very large metallicity (about 5 times the solar value) and one with no metals. The normalization of the two phases is roughly equal and the upper temperature limit is 2 keV.

magnitude as would approximately be required to bring the cooling flow prediction for this temperature phase in accord with the observed spectrum for M 87, the apparent metallicity for the bulk temperature of 1.1 to 1.6 keV in the inner cooling flow region would also be a factor of 2 to 4 lower than the true metallicity. The metallicity increase towards the center would than be even more dramatic than already derived for a homogeneous metallicity distribution with an increase of the iron abundance by a factor of 2 to 3. This can be seen e.g. in Fig. 6 where the fit yields a metallicity of 5 times the solar value for the enriched phase, which has roughly half the emission measure. Secondly the suppression of the metal lines is an

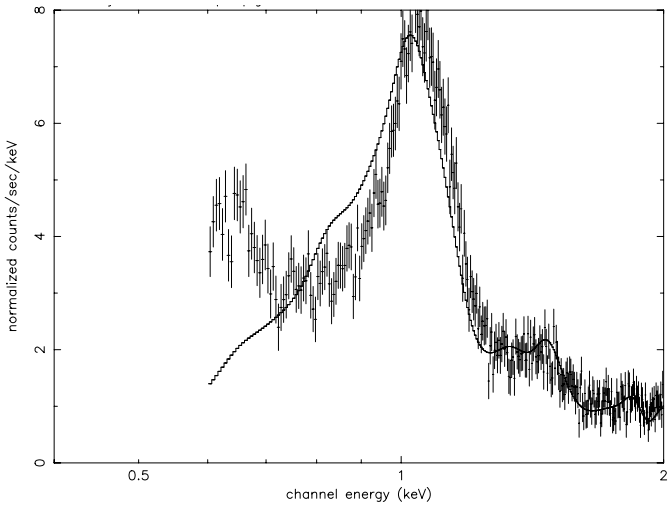

Fig. 7. *XMM EPN*-spectrum of the central region of the M 87 halo as shown in Fig. 2, now fitted with a cooling flow model and a free parameter for the internal excess absorption. The spectrum was constrained to the temperature interval 0.6 to 2.0 keV.

effect which gradually increases with decreasing temperature, so that if strong Fe L-shell lines are observed at 1.1 to 1.6 keV they will not suddenly disappear from the spectrum at a slightly lower temperature. Thus we would still expect to observe a considerably broadened iron L-shell peak, as was shown in Matsushita et al. (2001). We show this effect also here in Fig. 6 for the example of the X-ray emission from the $r = 1'-2'$ ring in M 87. The spectral iron feature is clearly not consistent with the observed spectrum. Since we consider these examples as representative of the general solution of the problem with a variety of possible mixing distributions of the metal abundances, we do not expect that the general discrepancy can be resolved by adopting a chemically inhomogeneous intracluster medium (at least for this detailed observation of M 87).

3. The interpretation of cooling flow spectra and cluster intrinsic absorption

Another possible way to make the observed Fe-L line feature roughly consistent with a cooling flow model is to allow the absorption parameter in the fit to adjust freely. This is demonstrated in Fig. 7 where we have again taken our example spectrum of the annular region in the M 87 halo. Now we have limited the spectral range to be fitted to energies above 0.6 keV and taken the absorption column density as a free fit parameter. In order to match the Fe-L peak shape better, the best fitting absorption column density is selected in such a way by the fit that the absorption edge limits the extent of the Fe-L line feature towards lower energies.

This is actually a good representation of the spectral fitting of cooling flow models that have been performed on *ASCA* data. For *ASCA* the sensitivity for the low energy part of the spectrum was much less than for *XMM-Newton*

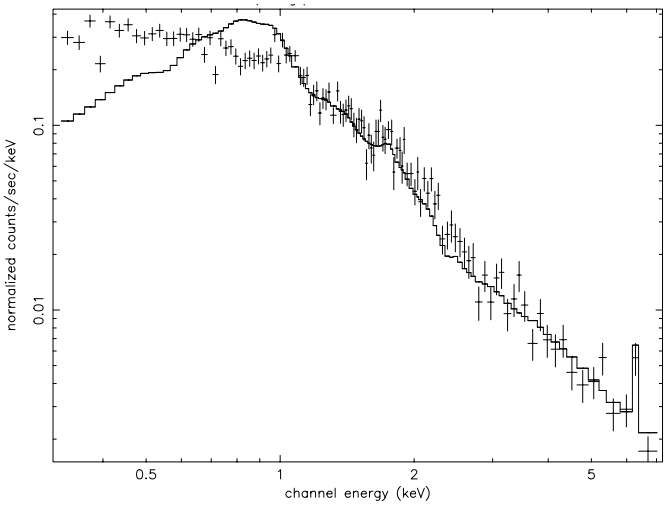

Fig. 8. *XMM EPN*-spectrum of the central region of the cluster A1795 fitted by a cooling flow model with a mass deposition rate of 50 $M_\odot$ yr^{-1} and an additional hot component at a temperature of 5.2 keV. The value for the absorbing column density was set to the galactic value of 1.26×10^{20} cm^{-2}.

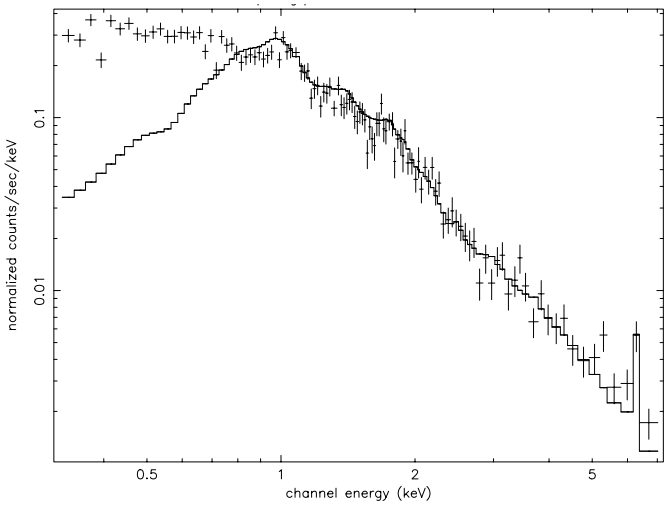

Fig. 9. *XMM EPN*-spectrum of the central region of the cluster A1795 fitted by a cooling flow model with a mass deposition rate of 50 $M_\odot$ yr^{-1} and an additional hot component at a temperature of 5.2 keV. The value for the absorbing column density of 3×10^{21} cm^{-2} was chosen to obtain an approximate fit to the narrow iron L-shell line feature.

and this spectral energy range was not very well calibrated. Therefore, in general the spectral part below about 0.6 to 0.7 keV was not included in the fit (e.g. Allen 2000; Allen et al. 2001), just as in our example. Therefore the *ASCA* experience has left us with two possible options of the interpretation of the spectra of cooling core regions: (1) an interpretation of the results in the form of an inhomogeneous cooling flow model which than necessarily includes an internal absorption component (e.g. Fabian et al. 1997; Allen 2000; Allen et al. 2001), or (2) an explanation of the spectra in terms of a two-temperature component model (e.g. Ikebe et al. 1997, 1999; Makishima 2001) where the hot component is roughly equivalent to the hot bulk temperature of the clusters and the cool component corresponds approximately to $T_{\rm low}$. As actually pointed out e.g. in Ikebe et al. (1999) and also seen in Allen et al. (2001) the two-temperature models provided in almost all cases a slightly but significantly better fit to the spectra as measured by the χ^2 statistic.

This phenomenon is not limited to the case of M 87, even though this is by far the best case where things can be demonstrated in the most obvious way, mostly due to the good (absolute) spatial resolution and photon statistics of this observation. In Figs. 8 and 9 this effect is illustrated for the cooling core region of the hotter and much more massive cluster A1795 which also harbours a much stronger cooling flow (e.g. Perez et al. 1998). Figure 8 shows the fit of a standard cooling flow model (with a very moderate cooling flow of only 50 $M_\odot$ yr^{-1} compared to the value of $\sim$340$-$750 $M_\odot$ yr^{-1} deduced from the imaging data by Peres et al. 1998) without absorption. Again we note a broad Fe-L line feature from the cooling flow model which is not observed. This feature is constraint to a narrower peak in Fig. 9 due to the inclusion of an internal absorption component of the order of 3×10^{21} cm^{-2}.

Thus there is a combination of the effects of internal absorption and the signature of cooling flows which can be interpreted as a suspicious coincidence or as a reconfirmation of the cooling flow model due to the detection of the cold material sink. We have seen in the above examples that in order to produce a sharp Fe-L line feature the absorption edge has to appear at the right energy and therefore values for the absorption column of typically around 3×10^{21} cm^{-2} are needed (for nearby clusters). Values of this order are actually found in most of the cooling flow model fits. For example Allen (2000) and Allen et al. (2001) find in recent improved *ASCA* studies indeed values in the range $1.5{-}5 \times 10^{21}$ cm^{-2}.

Contrary to the case of *ASCA*, the *XMM-Newton* data can be analysed to lower energies and the presence of the strong soft continuum component (including the oxygen Lyα line in the case of M 87) indicates that absorption may not be present or is affecting only the cold and dense part of the cooling core plasma. Therefore it is very important to test the case of internal excess absorption in an independent way. This is now possible for the first cases thanks to the *XMM-Newton* and *Chandra* observatories, as explained in the next section.

4. Non-detection of sufficient internal absorption in two test cases

To perform a test on the presence of absorbing material in the central regions of clusters independent of the complex fitting of multi-phase intracluster medium emission models, we need an independent light source. This fortunately exists in the form of the emission from the central AGN in many cooling flow clusters (e.g. Burns 1990). For example in the case of M 87 we can now obtain spatially resolved spectra of the nucleus and the brightest knot in

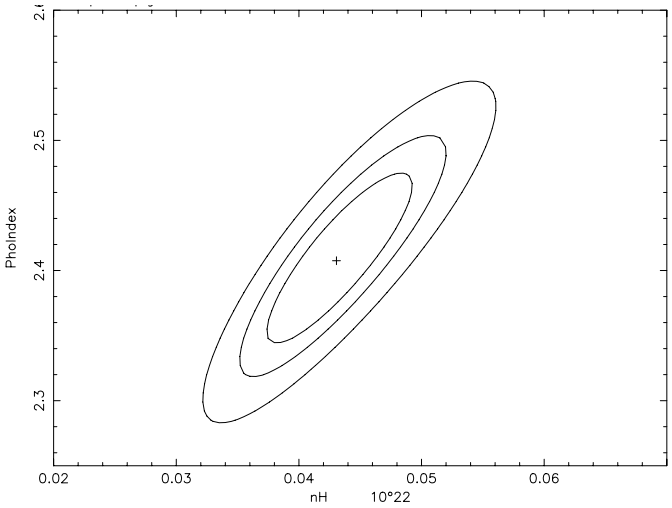

Fig. 10. Constraints on the shape of *XMM EPN*-spectrum of the nucleus of M 87. The lines show the 1, 2, and 3σ confidence intervals for the combined fit of the slope (photon index) of the power law spectrum and the value for the absorbing column density, $n_{\rm H}$.

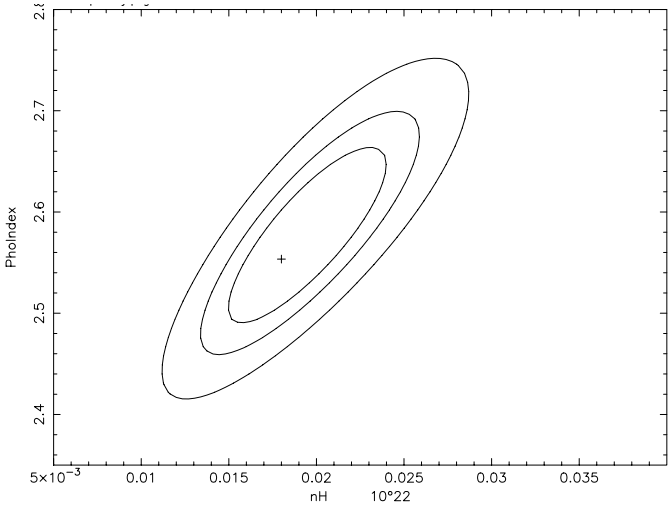

Fig. 11. Constraints on the shape of *XMM EPN*-spectrum of the brightest knot in the jet of M 87. The lines show the 1, 2, and 3σ confidence intervals for the combined fit of the slope (photon index) of the power law spectrum and the value for the absorbing column density, $n_{\rm H}$.

the jet with the high collecting power of *XMM-Newton* (Böhringer et al. 2001). These spectra can be fitted quite well with a power law spectrum and nearly galactic absorption. In Figs. 10 and 11 we show the combined constraints on the power law slope and the absorbing column density from the spectral fits. The 2σ upper limit on the excess absorption has a value of about 5×10^{20} cm^{-2}, almost one order of magnitude lower than what is required for a successful cooling flow spectrum fit.

Similarly, the central AGN in NGC 1275 in the center of the Perseus cluster is resolved with *Chandra* and we can obtain a spectrum from this point source (from the Perseus observation data in the *Chandra* archive) as

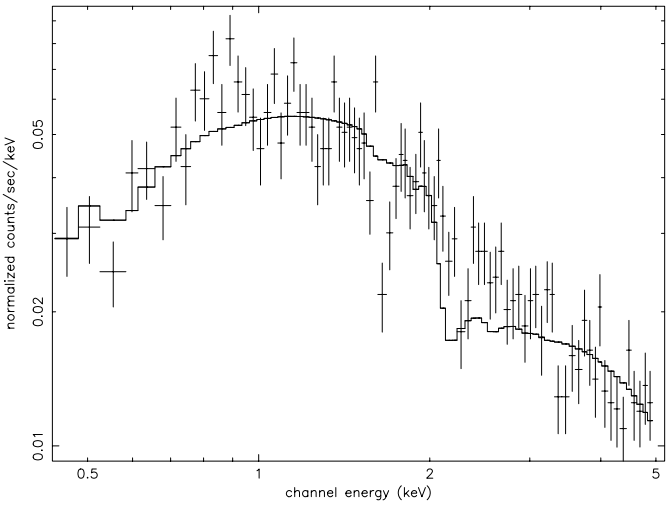

Fig. 12. *Chandra*-spectrum of the nucleus of NGC 1275 fit by a power law spectrum and a free fitting parameter for the absorbing column, for which a best fitting value of about 6×10^{20} cm^{-2} was found.

shown in Figs. 12 and 13. These spectra are much noisier than those for M 87 due to the lower photon statistics. The best fitting value for the absorbing column density is even slightly lower than the galactic value. An absorption column of more than 3×10^{21} cm^{-2}, as needed for a successful fit of the cooling flow model, is clearly inconsistent with the observations. There is some concern that the spectrum of the NGC 1275 nucleus is affected by photon pile up in the CCD pixels. The count rate for the nuclear emission is about 0.07 counts s^{-1}, quite low, however, and according to the *Chandra* Handbook the effect is in the percent range which cannot explain the large difference between the high absorption fit and the observed spectrum. This is all the more true as the effect is expected to result in low energy photons being sometimes bunched together and registered as events of higher energy, thus reducing the low energy flux by mimicking a higher absorption, which is not found in the observations.

Hopefully this test can be extended to further cooling core regions by means of *XMM-Newton* and *Chandra* to see if this conclusion can be reached in general. Nevertheless these two test cases indicate that the agreement of the cooling core spectra with the inhomogeneous cooling flow model plus excess absorption may have been obtained through a fortunate conspiracy of the two effects and the new results (including the RGS, EPN, and MOS spectra for a number of clusters) no longer support this interpretation. In one further case, in Hydra A, the spectrum of the central nucleus has been resolved and recorded. Unfortunately in this case a very high absorption value in excess of 10^{22} cm^{-2} has been found (McNamara et al. 2000) which has to originate very close to the nucleus and is not caused by the cooling core region. But due to the high AGN intrinsic absorption it does not allow us to probe the possible lower absorption of the cooling flow.

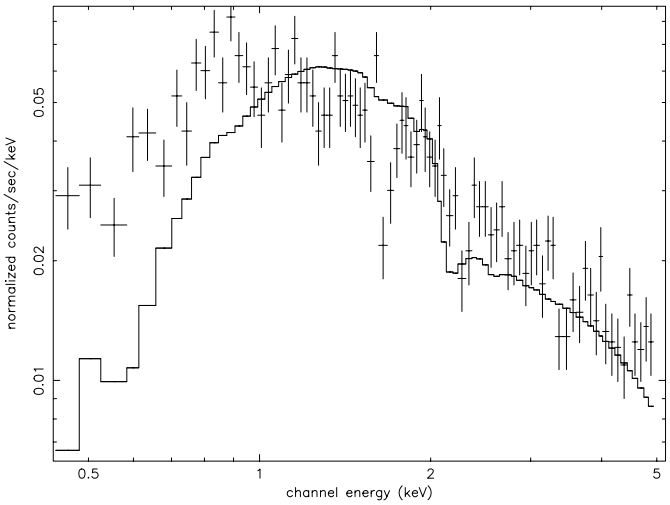

Fig. 13. *Chandra*-spectrum of the nucleus of NGC 1275 fit by a power law spectrum and a fixed fitting parameter for the absorbing column density of 3.3×10^{21} cm^{-2} as approximately needed in the fits of cooling flow models to *ASCA* spectra of NGC 1275.

There is still another argument left to save the absorption picture, which is a partial covering model, where the absorption would only be effective in the line-of-sight of the cold clumps. Even though this might be considered as an unwanted complication of the cooling flow model it should nevertheless be considered. Thus, let us assume that the absorbing material is only found in connection with cold condensing gas and let us again scale the model to the M 87 halo where we have the best observable parameters. If most of the hotter, visible plasma is confined to the temperature range 0.8 to 1.7 keV and the hidden plasma to temperatures below the lower limit of this range, the colder plasma will be approximately a factor of 2 denser and will cool about a factor of 4 faster (due to the higher density and the higher efficiency of the line cooling). The cool gas will than occupy a volume fraction of the order of 10%. Let us further assume that the enriched phase constitutes only about 40% of this cold plasma (a lower value would in the light of the above results lead to very high "true" metal abundances and thus we consider 40% as an extreme limit). Thus the material associated to the intrinsic absorption effect should at least have a filling factor of about 4%. Already the deep pointings on M 87 with the ROSAT HRI should have resolved cool clumps with kpc size in the surface brightness distribution of the M 87 halo image, thus these condensations must have a smaller scale. Taking the total line-of-sight through the cooling flow region starting at a cooling radius of about 50 kpc, we find that the optical depth for having clumps of kpc size in the line-of-sight towards the nucleus is about 2. Thus the chance that we have missed any absorbing column in the three tests with the nuclei of M 87 and NGC 1275 and the jet of M 87 is indeed small. Nevertheless, it will be very important to find further test cases.

5. Evidence for inhomogeneities and mass deposition in X-ray images

In view of the problems encountered above in the interpretation of the recent observational data in terms of a standard cooling flow model, we will explore in this section and the next one two more general aspects of the cooling flow model which hopefully will give further guidance to the interpretation of the observational results of cluster cooling cores: (i) observations of inhomogeneities in the inhomogeneous cooling flows and (ii) cooling flows in rotating clusters.

The inhomogeneous cooling flow model features a thermally unstable plasma in approximate pressure equilibrium where the cooling of the gas is accelerating when the gas is cooling. That is, temperature and density differences are magnified during the cooling process. Since initial density inhomogeneities are required to obtain an inhomogeneous cooling flow and since these inhomogeneities are continuously increasing in the comoving cooling flow model without heat exchange, we should expect that the cooling flow zone is characterized by a very inhomogeneous plasma. Inspecting some of the best observed cooling flow clusters, e.g. M 87, we find that the cooling flow regions actually have a quite regular X-ray appearance over most of the cooling flow region and in most cases they have elliptical symmetry reproducing the potential of the underlaying cD galaxy almost perfectly (e.g. Allen et al. 1995; Böhringer et al. 1997; Buote & Canizares 1994, 1996). We have sometimes argued in the past that this just reflects the fact that the inhomogeneities in the cooling flow have to appear on scales not yet resolved by the available X-ray imaging instruments and used this to set a lower limit on the suppression of classical heat conduction as required by the cooling flow model (e.g. Böhringer & Fabian 1989). Any detection of such inhomogeneous structure would help to guide us in the more realistic modeling of cooling flows.

A deeper inspection of some of the closest clusters observed with the *ROSAT HRI* and now with high resolution images taken with *Chandra* actually reveals inhomogeneous structure in the cluster cores. In Fig. 14 we show for example the *ROSAT HRI* image of the core region of the M 87 X-ray halo. The point sources originating from the M 87 AGN and the brightest knot in the jet have been removed from the image. One clearly notes that the X-ray emission is not symmetric around the AGN, which is most probably the gravitational center of the cD galaxy M 87. The surface brightness distribution can be interpreted as a region of diffuse excess emission in the North of the nucleus (Böhringer 1999).

A quite similar surface brightness excess region is found in the *ROSAT HRI* and *Chandra* images of NGC 1275 towards the SE of the nucleus of this galaxy (Böhringer et al. 1993; Fabian et al. 2000). In the case of M 87, the analysis of the X-ray hardness distribution in the *XMM-Newton* data indicates that this excess

region is colder than the surroundings (Matsushita et al., in preparation) and for the bright blob in NGC 1275 the *Chandra* data indicate the same (Schmidt & Fabian 2001). Therefore these excess emission regions most probably are colder and denser blobs. They could be inhomogeneities in which material is presently cooling and condensing in the cooling cores of these clusters. Further evidence for such inhomogeneities is now coming from many high resolution images of cluster cooling cores of nearby clusters which can be well enough resolved with *Chandra*. In A1795 for example a cooling tail has been found with a length of about 80 h_{50}^{-1} kpc and temperatures in the range 2–3 keV, cooler than the ambient medium (Fabian et al. 2001b). The X-ray filament coincides with an emission line filament observed in Hα+NII (Cowie et al. 1983). In Hydra A McNamara et al. (2000) observed a flattened excess X-ray emission structure which is coincident with a gaseous star-forming disk with an estimated star formation rate between 1 and 15 $M_\odot$ yr^{-1} (depending on the duration of the assumed star burst $\sim 10^9$ or 10^8 yr, respectively, McNamara et al. 2000). Also in A1835 an excess emission region close to the center and inhomogeneities are observed. These features are well inside the optical central galaxy of the cluster (Schmidt et al. 2001).

The common feature of almost all these detections of inhomogeneities is that these features are found in the very central region of the cooling flow, most often inside the optical image of the central cD galaxy. The filament in A1795 with a length of 80 h_{50}^{-1} kpc is among these examples by far the largest off-center structure. Thus we note that these inhomogeneities are generally found only in the centers of cooling flows and most of the much larger cooling flow region (with radii from 50 kpc to over 200 kpc for the above examples, see Peres et al. 1998; Schmidt et al. 2001) is generally more regular.

Taking these features as a manifestation of actually cooling and condensing gas we find that the mass deposition rates calculated for these localized regions are (of course) much smaller than what is inferred for the entire cooling flow. In the case of the bright blob north of the center of M 87 we find a steady state mass deposition rate in the blob if it is cooling without disturbance of a few tenths of a solar mass per year, while for the bright blob in NGC 1275 the estimated mass deposition rate is of the order of 10 solar masses per year. Thus, mass deposition, where we can supposedly observe it directly, is one or two orders of magnitude less than what has classically been claimed for the cooling flow mass deposition. If steady state cooling would be reduced to these low values, there would be no conflict with the interpretation of the spectroscopic results since in most cases a cooling process is consistent with the data if the mass deposition rate is reduced by at least one order of magnitude with respect to the conventional cooling flow value (see e.g. Matsushita et al. 2001 for the case of M 87 where a mass deposition rate of up to 1 $M_\odot$ would be consistent with the data).

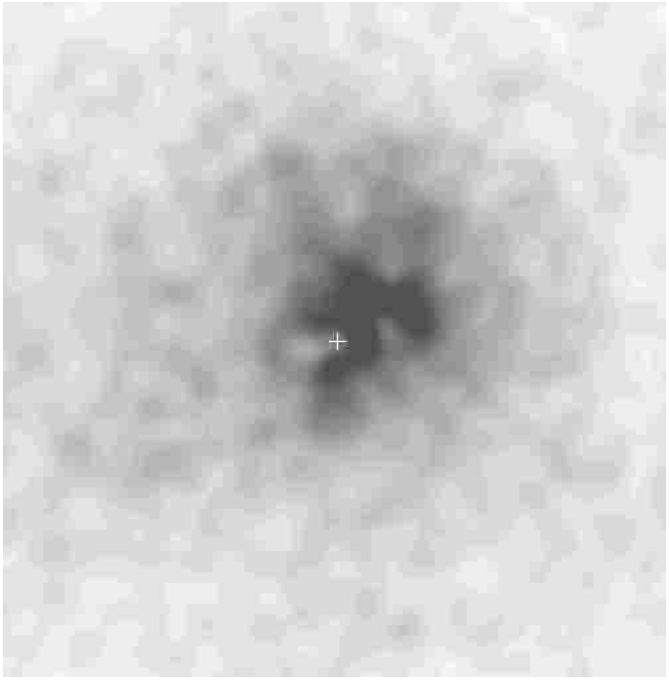

Fig. 14. X-ray morphology of the central part of the M 87 halo as observed with the *ROSAT HRI*. The two point sources originating from the central AGN and the brightest knot of the jet have been subtracted. The position of the nucleus of M 87 is marked. The scale of the image is 2.13×2.13 arcmin^2. The X-ray emission is clearly not symmetric around the galactic center of M 87 and there is an obvious emission excess towards the North of the nucleus where also emission line filaments are observed.

Lower mass deposition rates in cooling flows have been advocated previously by a number of authors e.g. O'Dea (1994), Braine et al. (1995), Voit & Donahue (1995), McNamara et al. (2000), mostly to bring the results into consistency with the observations of optical emission lines and indications of star formation. Even the very recent observations of large amounts of warmed molecular gas are not necessary calling for very high mass deposition rates. For 34 clusters observed by Edge (2001), only 7 extreme cooling flow clusters show mass estimates for the cold gas from CO line observations in excess of 3×10^{10} $M_\odot$, most of which have inferred mass deposition rates of 1000 $M_\odot$ yr^{-1} and more. Thus, if the gas observed in CO is the final cold sink it could still be explained by mass deposition rates reduced by an order of magnitude and for the smaller inferred gas mass values stellar mass loss could even be an important contribution.

6. Problems of cooling flows in rotating clusters

The effect of cluster rotation (or the rotation of elliptical galaxies) on cooling flows has been considered in several works (e.g. Kley & Mathews 1995; Garasi et al. 1998). Since we have not yet found much direct evidence for cluster rotation, the implications of these studies have not generally been integrated into the cooling flow picture. We approach this problem here from the general perspective

of structure formation in the Universe from which statistical predictions for the degree of rotation to be expected for clusters are obtained and then discuss the implications for massive cooling flows.

Simulations of the evolution of structure provide predictions for the typical spin parameter, λ, of dark matter halos, e.g. in the scale-free simulations of Efstathiou et al. (1988) with values of about $\lambda = 0.04 - 0.06$ (where the spin parameter is defined as $\lambda = J\,|E|^{1/2}\,G^{-1}\,M^{-5/2}$; see also e.g. White 1996 for an overview). Efstathiou et al. (1988) also provide the more practical values of the ratio of the rotational velocity to the velocity dispersion e.g. for the region where the overdensity is about 500 of the critical density of the Universe, with a value of about 0.15. In galaxy clusters this rotation has not been observed directly but it has been investigated in detail for giant elliptical galaxies which constitute smaller dark matter halos which can be viewed as scaled down versions of clusters. In a study of 22 ellipticals with a mean velocity dispersion of about 250 $\mathrm{km\,s^{-1}}$ by Franx et al. (1989) they find a mean rotational velocity of about 52 $\mathrm{km\,s^{-1}}$ which is slightly larger but roughly consistent with the value of about 15% found in the simulations. The slightly higher value actually provides some margin to include some energy dissipation and matter segregation in this case.

In the case of M 87 there is actually some weak indication for large-scale rotation of the dark matter halo from the velocity distribution of the globular cluster system associated to this giant elliptical. Some indication for rotation was found by Sembach & Tonry (1996) and Mould et al. (1990). In a recent study of the velocity distribution of 205 globular clusters in M 87 these earlier indications were confirmed and improved by Cohen & Ryzhov (1997). Even so, the scatter in the data is large, the best fitting model gives a significant rotation with a rotational velocity of the order of 100 $\mathrm{km\,s^{-1}}$ roughly in the direction of the PA 140 ($\pm$30) deg for a mean radius of about 15 kpc. This would, compared to the velocity dispersion in the larger dark matter halo of the Virgo cluster (in early type galaxies) with a value of about 550 to 600 $\mathrm{km\,s^{-1}}$, be again consistent with the ratio of rotational to random velocities in the inner region of the Virgo cluster.

To see how this affects the structure of cooling flows, let us start with a model for M 87 and then draw general conclusions. In M 87 the cooling radius for a cooling time of 10 Gyr is at about 55 kpc. Thus we take a radius of about 50 kpc to start the cooling flow. For this radius we calculate a Keplerian velocity of 720 $\mathrm{km\,s^{-1}}$ and the observed velocity dispersion for early type galaxies which trace the cluster potential best has the value quoted above. With the ratio of the rotational velocity to the velocity dispersion of about 0.15 we find a typical expected rotational velocity of about 82 $\mathrm{km\,s^{-1}}$. If the cooling flow starts with this rotation and flows inward under conservation of angular momentum, the flow will be rotationally supported when it reaches a radius of about 11 kpc when the Keplerian velocity estimated from the mass profile derived by Matsushita et al. (2001) is about 375 km $\mathrm{s^{-1}}$. At this radius we expect an accretion disk to be formed. Due to the angular momentum that will be transported outwards it should also extend to slightly larger radii. Thus in M 87 the accretion disk should at least have a radius of about 12 kpc (2.4 arcmin). Inspecting Fig. 14, there is no signature of a rotationally supported gas disk of this size. If we take the rotation of the globular cluster system as a guide we should expect the disk to be oriented roughly along PA 140 deg.

The general case for any cluster will be similar to the case of M 87 where the cooling radius of about 50 kpc is probably also close to the dark matter core radius. In general one finds cooling radii in the range of about 0.5 to 1 times the estimated gravitational core radius. At the core radius the Keplerian velocity is very close to the velocity dispersion of the system (see e.g. King type models described in Binney & Tremaine 1997). Starting with a rotational velocity of 15% of the Keplerian velocity at the cooling radius and with the spinning up of the flow with decreasing radius, Keplerian velocity will be reached with less than a fivefold decrease in radius. Note that the Keplerian velocity decreases with decreasing radius inside the core radius of the dark matter potential. For cooling radii in the range of 50–150 kpc as found for massive cooling flows this should generally result in the formation of rotationally supported disks with sizes of at least 10 to 30 kpc.

In the simulation studies of cooling flows in rotating systems by Kley & Mathews (1995) and Garasi et al. (1998) flattened disks of hot gas were found, as expected. In both simulations the X-ray appearance was explicitly calculated and very flattened X-ray surface brightness distributions were predicted. These disks should be observable in the nearby clusters with high resolution X-ray imaging devices, at least in cases where they are seen edge on. Those features have not yet been observed in general, however, and we conclude that rotationally supported disks are not a general phenomenon in cooling flows as would be expected.

Indications of some trace of rotation has possibly been observed in the center of the Perseus cluster, were a spiral feature in the X-ray surface brightness distribution (Churazov et al. 2000) may indicate that we are looking at a rotating structure face on (see also Fabian et al. 2000). Also in Hydra A a small rotational structure of emission line gas has been observed (e.g. Heckman et al. 1985). But with the exception of Pereus perhaps, large rotational structures are not observed in general.

7. Heating model

Most of the problems in the interpretation of the observational results in terms of classical cooling flow models mentioned above, e.g. (i) the inconsistencies of the spectral models with the observed spectra, (ii) the lack of signatures of massive mass deposition at the degree predicted by the cooling flow model from image analysis at other wavelengths than X-rays and the lack of strong enough

star formation indices, (iii) the problem of angular momentum in massive flows, can be avoided if the flow and the mass deposition is reduced to a much smaller level than previously thought. The reduction should at least be about one to two orders of magnitude.

To reduce the mass condensation in the presence of energy conservation some form of heating is clearly necessary to balance the radiation losses. In principle three forms of heating sources have been discussed in the literature:

- heating by the energy output of the central AGN (e.g. Pedlar et al. 1990; Tabor & Binney 1993; McNamara et al. 2000; Soker et al. 2001);
- heating by heat conduction from the hotter gas outside the cooling flow (e.g. Tucker & Rosner 1983; Bertschinger & Meiksin 1986);
- heating by magnetic fields, basically through some form of reconnection (e.g. Soker & Sarazin 1990; Makishima et al. 2001) where in the model of Makishima et al. the energy dissipated by the magnetic fields originates from the motion of the cluster galaxies.

The latter two processes depend on poorly known plasma physical conditions in the intracluster medium of the clusters and therefore most probably remain in their quantitative effect highly speculative. The energy output of the central AGN can be determined, however, and we can obtain very clear boundary conditions for our model. Therefore we concentrate in this paper on the exploration of central cluster AGN as a source for heating the cooling cores of clusters.

Before starting the discussion of possible models we can put forward some general considerations on the properties that a successful heating model should have to provide a consistent interpretation.

- the energy input has to provide sufficient heating to balance the cooling flow losses, that is about 10^{60} to 10^{61} erg in 10 Gyr or on average about $3 \times 10^{43} - 3 \times 10^{44}$ erg s^{-1};
- the energy input has to be fine-tuned. Too much heating would result in an outflow from the central region and the central regions would be less dense than observed. Too little heat will not reduce the cooling flow by a large factor. Therefore the heating process has to be self-regulated: mass deposition triggers the heating process and the heating process reduces the mass deposition;
- the energy deposition has to provide a global heating effect. Local energy deposition would result in local heating while the mass deposition can still go on in the less well-heated regions;
- the heating process has to preserve the observed entropy structure in the intracluster medium in the central regions of cooling core clusters, with an entropy profile decreasing towards the center. This rules out for example any model in which heat is transported to larger radii by classical convective transport driven by a decreasing entropy with radius;
- the heating process should preserve the observed strongly increasing metallicity gradients in cooling core clusters.

Table 1. Estimated energy output from the central AGN in M 87, NGC 1275 and the central galaxy of the Hydra A cluster. The input parameters are the bubble radius, $r_{\rm B}$, the ambient pressure, $P_{\rm th}$, and the Keplerian velocity at the bubble location, $v_{\rm K}$.

system	$r_{\rm B}$	$P_{\rm th}$	$v_{\rm K}$	$L_{\rm kin}$
M 87	8 kpc	10^{-10} erg cm^{-3}	460 km s^{-1}	1.2×10^{44} erg s^{-1}
NGC 1275	15 kpc	2×10^{-10} erg cm^{-3}	600 km s^{-1}	1×10^{45} erg s^{-1}
Hydra A	15 kpc	2.8×10^{-10} erg cm^{-3}	550 km s^{-1}	2×10^{45} erg s^{-1}

We will discuss briefly in the following how these five requirements can be met. In a paper in preparation by Churazov et al (2001b) this model will be worked out and discussed in more detail. For the modeling of the heating process we take our guidance from the detailed observations of the interaction process of the AGN radio lobes in M 87 and NGC 1275 with the intracluster medium of the Virgo and Perseus cluster, respectively, and derive important boundary parameters from these observations. The interaction model is based on the scenario of subsonically expanding and rising radio lobe bubbles which was developed by Churazov et al. (2000, 2001a).

First of all we check the first requirement concerning the overall energetics. The interacting radio lobe bubble model allows us to estimate the output of the AGN in form of kinetic energy of the relativistic plasma in the jets for typical time scales of several 10^7 yr. The energy estimate relies on a comparison of the bubble inflation and buoyant rise time as described in Churazov et al. (2000) and requires as observational input parameters the bubble size, $r_{\rm B}$, the ambient pressure, $P_{\rm th}$, and the Keplerain velocity at the bubble radius in the cluster, $v_{\rm K}$. Then an order of magnitude estimate of the energy output of the AGN can be obtained by the formula

$$L_{\rm kin} = 10^{45} \left(\frac{r_{\rm B}}{13 \text{ kpc}}\right) \left(\frac{P_{\rm th}}{2 \times 10^{10} \text{ erg cm}^{-3}}\right) \quad (4)$$

$$\times \left(\frac{v_{\rm K}}{700 \text{ km s}^{-1}}\right)^{-2} \text{erg s}^{-1}. \quad (5)$$

Table 1 shows the input parameters and the resulting output energies for the case of M 87-Virgo, Perseus, and Hydra A. The results for Perseus can also be found in Churazov et al. (2000). For M 87 we have used the parameters for the inner bubble taken from the X-ray deficit observed in the jet region of M 87 as shown by Böhringer et al. (1995). Similar estimates were found by Churazov et al. (2001a) from a comparison of the appearance of the rising bubbles with the hydrodynamic simulations. The input parameters for Hydra A are taken from McNamara et al. (2000). In these estimates we assume that the bubbles are on the verge to rise, thus the observed values are

strictly to be taken as lower limits. Since the radial expansion velocity of the bubbles decreases rapidly with time we will most probably observe the bubbles near to their largest radius and thus the true values are most probably close to these lower limits.

These values for the energy input have to be compared with the energy loss in the cooling flow, which is of the order of 10^{43} erg s^{-1} for M 87 and about 10^{44} erg s^{-1} for the Perseus cooling flow. Thus in these cases the first requirement is met, the energy input is larger than the radiation losses in the cooling flow for Perseus and the M 87 halo for at least about the last 10^8 yr.

We have, however, evidence that this energy input continued for a longer time with evidence given by the outer radio halo around M 87 with an outer radius of 35–40 kpc (e.g. Kassim et al. 1993; Rottmann et al. 1996). Owen et al. (2000) give a detailed physical account of the halo and model the energy input into it. They estimate the total current energy content in the halo in form of relativistic plasma to 3×10^{59} erg and the power input for a lifetime of about 10^8 years, which is also close to the lifetime of the synchrotron emitting electrons, to the order of 10^{44} erg s^{-1}. The power currently supplied by the inner jets is also of the order of 10^{44} erg s^{-1} according to the model by Owen et al. (2000). Thus, even though the sharp boundary of several features at different scales within the radio halo suggest that the energy supply was not exactly steady and one may be able to distinguish several episodes of higher activity, the observations also imply, that there was a typical mean energy input from the AGN in form of relativistic plasma of about 10^{44} erg s^{-1} for at least about 10^8 years.

The very characteristic sharp outer boundary of the outer radio halo of M 87, noted by Owen et al. (2000), which is observed similarly at three different radio frequencies, 74 and 330 MHz (Kassim et al. 1993) and 10.6 MHz (Rottmann et al. 1996) has some further very important implications. Owen et al. (2000) already noted that this excludes the feeding of the halo by single-particle diffusion which would not lead to a sharp edge and not with the same location at all frequencies. Similarly, they argue that this speaks against an outflow, since this would lead to a more rapid radial dimming of the halo than observed. In a similar way we can argue, that it is difficult to produce such a sharp outer boundary (which looks even a bit edge-brightened) in a cooling flow by advection and compression of an ambient magnetic field associated with relativistic particles (as argued by Soker & Sarazin 1990, see also Fabian 1994). As a result of a cooling flow advection and compression we would expect a halo that gradually increases in brightness inwards, contrary to what is observed.

The best explanation of the radio halo morphology is provided by the rising radio bubble picture of Churazov et al. (2000, 2001a) in which the halo is filled with buoyantly uplifted bubbles which mix with ambient gas until they are loaded enough to find a hydrostatic equilibrium position in the M 87 halo. The typical hights that can be reached as calculated and simulated by Churazov et al. are in very plausible agreement with the observed size of the outer radio halo. (This model depends on the assumptions made for the mixing of the thermal and relativistic plasma – if contrary to the assumptions the mixing is not tight, the relativistic bubbles could subsequently leave the cooling flow region.)

In summary, we find a radio structure providing evidence for a power input from the central AGN into the halo region of the order of about ten times the radiative energy loss rate over at least about 10^8 years (for this representative example of M 87). The energy input could therefore balance the heating for at least about 10^9 years if all the input energy is used to heat the cooling flow region. The observation of active AGN in the centers of cooling flows is a very common phenomenon. Burns (1990) and Ball et al. (1993) find in a systematic VLA study of the radio properties of cD galaxies in cluster centers, that 71% of the cooling flow clusters have radio loud cDs compared to 23% of the non-cooling flow cluster cDs. Therefore we can safely assume that the current episode of activity was not the only one in the life of M 87 and its cooling flow.

Since similar central radio halos have so far been found at least in a number of other nearby cooling flow clusters, e.g. Perseus (Pedlar et al. 1990; Burns et al. 1992), A2199 (Owen & Eilek 1998), A133, A2052, A2626 (Rizza et al. 2000; Zhao et al. 1993), the scenario described above for M 87 should apply similarly to these cooling flow clusters.

Having demonstrated that the first requirement seems to be fulfilled, we can explore how a self-regulation mechanism might work, that adjusts the energy supply from the AGN to the cooling losses. This mechanism should most probably be searched for in a feeding mechanism of the AGN by the cooling flow gas, as generally suggested in most models that featured AGN heating. The most simple physical situation would be given if simple Bondi type of accretion from the inner cooling core region would roughly provide the order of magnitude of power output that is observed and required. Using the classical formula for spherical accretion from a hot gas by Bondi (1952) we can obtain a very rough estimate for this number. For the proton density in the environment of the M 87 nucleus we find an average value of about 0.1 cm^{-3} over a region of about 15 arcsec radius and a temperature of about 10^7 K from the *XMM-Newton* observations (Matsushita et al. 2001). Thus for a black hole mass of 3×10^9 $M_\odot$ (e.g. Ford et al. 1994; Macchetto et al. 1997) we find a mass accretion rate of about 0.01 $M_\odot$ yr^{-1} and an energy output of about 7×10^{43} erg s^{-1}, where we have assumed the canonical value for the ratio of the rest mass accretion rate to the energy output, that is the energy conversion efficiency. For the accretion radius, which we approximately take as the radius where the Keplerian velocity in the potential of the black hole is equal to the sound speed, we find approximately a value of 50 pc ($\sim$0.6 arcsec). That we get with this very crude estimate so close to the required energy output is extremely encouraging. We should note further, that the required accretion rate with an energy output

of 10^{44} erg s^{-1} is more than a factor of 1000 below the Eddington accretion rate and thus no reduction effects of the spherical accretion rate by radiation pressure have to be expected. We should further note that in this model small changes in the temperature and density structure in the inner cooling core region will directly have an effect on the accretion rate. Therefore we have all the best prospects for building a successful self-regulated AGN-feeding and cooling flow-heating model. This will be discussed further in the paper by Churazov et al. (2001b).

We have listed as a third requirement for the heating model the fact that the heating must be global to the whole cooling flow region. If the heating would be acting only on certain regions of the plasma, they would be heated and get buoyant while the rest of the plasma would still feature a cooling flow. In the most extreme case this would lead to classical convection, which is excluded by the observations of the observed entropy structure.

To explore the heating process further we shall consider how the energy is transferred from the relativistic plasma in the bubbles to the thermal intracluster medium in the frame of the rising bubble model of Churazov et al. (2000, 2001a). In fact most of the primary energy input from the jets is transferred to the thermal plasma in form of adiabatic work spent on the surrounding medium. 25% of the energy is lost directly from the relativistic plasma during the inflation of the bubbles. Further, about 45% are transferred to the ambient medium during the adiabatic expansion of the bubbles if they rise from about 1 kpc to 40 kpc featuring a pressure drop of about a factor of 10. Thus more than half of the energy is transferred in a global way by PdV-work done on the ambient medium. Since the bubbles are expanding subsonically (at least on average) this energy will be converted into sound waves, gravity waves, and in the very plausible case of an unsteady expansion of the bubbles into low amplitude shock waves. How much of this energy can be deposited in the cooling flow region and how the energy is spread in detail over the region remains to be explored in detail. Two points are nevertheless noteworthy. The energy is not deposited directly in the boundary of the bubbles, as it would be expected for supersonic expansion. This is consistent with the observations where the gas directly bounding the bubbles seems colder than the general medium in the cooling cores (Schmidt & Fabian 2001). Part of this energy should be dissipated in the cooling flow region, in particular if low amplitude shock waves are involved, and we may not need a 100% efficiency of the heating to reduce the cooling flow mass deposition, depending on the duty cycle of the on and off state of the central AGN.

Further energy input into the cooling flow region is gained from the uplift of gas dragged along with the rising relativistic plasma bubbles. During this interaction of the relativistic and thermal plasma the thermal gas will also be heated by dissipation of turbulence and reconnection of the magnetic fields in the Kelvin-Helmholtz instability interaction regions. Since in the model by Churazov et al. these rising bubbles of relativistic plasma and dragged ambient gas will finally reach a hydrostatic equilibrium position where they will expand laterally, this spreading will provide an effective energy distribution in the azimuthal direction helping to distribute the energy originated from the AGN globally in the cooling flow region. As noted above, the working of this model depends also on the way the thermal and relativistic plasma can mix. Again we refer to the more detailed modeling that will be presented in the following paper, but argue here that the prospects for fulfilling the third condition looks good under the circumstances described here.

The last two requirements noted, the consistency with the observed entropy structure and the metallicity increase towards the center, will not be met for example by a conventional heating model in which the thermal intracluster medium is mostly heated at the center and where a convectively unstable entropy profile that decreases with radius is driving the convective energy transport. The rising radio bubble model of Churazov et al. (2000, 2001a) is clearly different to this situation, since here a kind of convective transport is mediated by the relativistic plasma bubbles which uplift thermal gas without effective heating, at least in the central region. Support for this presumption in the case of M 87 comes from the observation, that the gas within the upstreaming relativistic plasma is colder than the ambient medium (Böhringer et al. 1995; Belsole et al. 2001). This is most probably explained by the fact that the uplifted gas expands adiabatically and cools. This is the so far best explanation at hand for the observation of the cooler thermal gas within the radio lobes. The adiabatic cooling effect has also been clearly found in the simulations of the rising bubble model by Churazov et al. (2001a).

Concerning the metal distribution, some simple estimates show that the abundance of the heavy elements in the central region (the inner about 10 kpc) can be replenished by the effect of supernovae type Ia and by stellar winds within about 2 Gyrs (see also Matsushita et al. 2001). Even the case of a cooling flow with slow enough inflow velocities is not strongly violating the time scale requirements for this to happen. Therefore slow convection flows driven by the radio bubbles will most probably be also consistent with the abundance distribution profiles. The available X-ray observations provide more details for the guidance of further modeling in this direction that we plan to use for future work.

8. Magnetic fields

Large Faraday rotation measures have been found in cooling flow clusters with values of a few 100 up to 8000 rad m^{-2} (Dreher et al. 1987; Owen et al. 1990; Burns et al. 1992; Taylor & Perley 1993; Ge & Owen 1993; Taylor et al. 1994; Taylor et al. 2001) indicating that strong magnetic fields exist in these cooling core regions of clusters. Previously these magnetic fields were attributed to the advection and compression of magnetic flux and associated relativistic particles in the cooling flows predicted to

reach field strengths up to the equipartition value (e.g. Soker & Sarazin 1990). These signatures were also taken as a reconfirmation of the cooling flow picture that makes the amplification of the magnetic fields possible (Fabian 1994).

Taking again the case of M 87 as an example, the sharp outer boundary of the outer radio lobes is not much in favour of such a model, as discussed above. The strong magnetic fields could alternatively result from plasma accumulation from the rising radio lobe bubbles. When the radio synchrotron emitting electrons have long lost their energy the associated magnetic field will still persist. To observe in this case strong Faraday rotation measures poses another constraint on the mixing model of the rising radio lobe bubbles. The magnetic field has to mix with the thermal plasma, since the observed rotation measure depends on the product of the magnetic field strength and the electron density. If such a mixing is possible is unclear at this stage and it might be difficult to predict theoretically. (One could ask in a similar way if the observed about 10% influx of the solar wind magnetic field into the magnetically separated magnetosphere would have been predicted on purely theoretical grounds were there no observational indication that this has to happen). Again we have to hope for observational signatures that could possibly guide our further modeling.

Nevertheless it is interesting to speculate somewhat further. Since the sharp boundary of the larger M 87 radio halo is so intriguing, and since we observe these strikingly sharp features of so-called cold fronts in merging clusters (Markevitch et al. 2000; Vikhlinin et al. 2000; Mazotta et al. 2001) we may wonder, if the separation of the material inside the cold front from the ambient medium is produced by the magnetical structure of a fossil radio halo produced by the convective radio bubble model of the AGN heating of a cooling core region. This suggestion would naturally provide a sharp boundary for the cold front structure. Support for this suggestions would be provided if a jump in the magnetic field strength could be detected across the cold front.

9. Conclusions

Several observational constraints have let us to the conclusion that the mass deposition rates in galaxy cluster cooling cores are not as high as previously predicted. The new X-ray spectroscopic observations with a lack of spectral signatures for the coolest gas phases expected for cooling flows, the morphology of the X-ray surface brightness distribution in the cooling flows, and the lower mass deposition rates indicated at other wavelength bands than X-rays are more consistent with mass deposition rates reduced by one or two orders of magnitude below the previously derived values. This can, however, only be achieved if the gas in the cooling flow region is heated. While the cooling flow models, governed essentially by the energy equation without a heating term, were in fact the most simple possible description, it seems now that we have to add a step of complication and introduce an additional heating process. The most promising heating model is most probably a self-regulated heating model powered by the large energy output of the central AGN in most cooling flows.

Most of the guidance and the support of the heating model proposed here (based on concepts developed in Churazov et al. 2000, 2001a) is taken from the detailed observations of a cooling core region in the halo of M 87 and to a smaller part from the observations in the Perseus cluster. These observations show that the central AGN produces sufficient heat for the energy balance of the cooling flow, that the most fundamental and classical accretion process originally proposed by Bondi (1952) provides an elegant way of devising a self-regulated model of AGN heating of the cooling flow, and that most of the further requirements that have to be met by a heating model to be consistent with the observations can most probably be fulfilled.

Since these ideas are mostly developed to match the conditions in M 87, it is important to extent such detailed studies to most other nearby cooling flow clusters. The same model does not necessarily work in all cases. In some clusters more violent, supersonically expanding radio lobes may have to be taken into account (e.g. for Cyg A). The study of a sample of cooling flow clusters could also provide important insight into the duty cycle of the AGN activity and the feedback mechanism.

In this new perspective the cooling cores of galaxy clusters become the sites where most of the energy output of the central cluster AGN is finally dissipated. Strong cooling flows should therefore be the locations of AGN with the largest mass accretion rates. While in the case of M 87 with a possible current mass accretion rate of about 0.01 $M_\odot$ yr^{-1} the mass addition to the black hole (with an estimated mass of about 3×10^9 $M_\odot$) is a smaller fraction of the total mass, the mass build-up may become very important for the formation of massive black holes in the most massive cooling flows, where mass accretion rates above 0.1 $M_\odot$ yr^{-1} become important over cosmological times.

Note added in proof: A model for the interaction of buoyantly rising relativistic plasma bubbles with the intracluster medium and the interruption of cooling flows is also described in recent work by Quilis et al. (2001) providing similar conclusions as the work by Churazov et al. (2001) outlined above.

Acknowledgements. We like to thank Rashid Sunyaev, Andrew Fabian, and Peter Schuecker for valuable comments. The paper is based in some parts on observations obtained with XMM-Newton, an ESA science mission with instruments and contributions directly funded by ESA Member States and the USA (NASA). The XMM-Newton project is supported by the Bundesministerium für Bildung und Forschung, Deutsches Zentrum für Luft und Raumfahrt (BMBF/DLR), the Max-Planck Society and the Haidenhain-Stiftung.

Appendix A

In this appendix we derive the formula to calculate the apparent metallicity for a mixed phase plasma as used in Sect. 2.2. In the following calculations we argue in terms of the total metal abundance as a unique value, but the derivation can directly be generalized to any metal element abundance distribution as long as different metal element abundances are kept fixed for both phases for the whole temperature range considered. Before we can start the calculations we need a reference for the fraction of power radiated by metal lines (and the continuum contribution from metals through e.g. recombination) compared the fraction of the continuum radiated by a plasma devoid of metals. We calculate this reference function for the case of a plasma with solar abundances as a function of temperature (using XSPEC) to define the function $\mathcal{F}_1$, which gives the metal line fraction to the total radiation for solar metallicity plasma. This function $\mathcal{F}_1(T)$ is shown in Fig. 4. The function can be transformed to calculate the metal line fraction for any other metallicity value, e.g. the metallicity of the enriched phase of the example in Sect. 2.2. by the formula

$$\mathcal{F}_2 = \frac{z_2 \mathcal{F}_1}{z_2 \mathcal{F}_1 \ + \ (1 - \mathcal{F}_1)}. \tag{A.1}$$

The apparent metallicity, $z_{\rm obs}$, is then equal to the ratio of the observed radiation power in metal lines compared to the metal-devoid continuum in relation to the same parameters for the solar metallicity plasma

$$z_{\rm obs} = \frac{P_{\rm lines}}{P_{\rm cont.}} \times \frac{1 - \mathcal{F}_1}{\mathcal{F}_1} = \frac{f \ \mathcal{F}_2}{f \ (1 - \mathcal{F}_2) \ + \ (1 - f)} \frac{1 - \mathcal{F}_1}{\mathcal{F}_1}, \tag{A.2}$$

where f is the mass fraction of the enriched plasma phase. With some algebra (using the fact that $z_2 = z f^{-1}$) this can be transformed into

$$z_{\rm obs} = \frac{z \ (1 - \mathcal{F}_1)}{1 \ + \ \mathcal{F}_1 \ (z f^{-1} - 1 - z)}. \tag{A.3}$$

This function is shown in Fig. 5. The dramatic decrease of the apparent metallicity is not only caused by the fact that the metallicity of phase 2 goes to saturation but also by the fact that the phase 1 is forced to radiate purely by continuum emission.

References

Allen, S. W. 1995, MNRAS, 276, 947
Allen, S. W., Fabian, A. C., Edge, A. C., Böhringer, H., & White, D. A. 1995, MNRAS, 275, 741
Allen, S. W. 2000, MNRAS, 315, 269
Allen, S. W., Fabian, A. C., Johnstone, R. M., Arnaud, K. A., & Nulsen, P. E. J. 2001, MNRAS, 322, 589
Anders, E., & Grevesse, N. 1989, Geochim. Cosmochim. Acta, 53, 197
Ball, R., Burns, J. O., & Loken, C. 1993, AJ, 105, 53
Belsole, E., Sauvageot, J. L., Böhringer, H., et al. 2000, A&A, 365, L188
Bertschinger, E., & Meiksin, A. 1986, ApJ, 306, L1
Binney, J., & Tremaine, S. 1987, Galactic Dynamics (Princeton University Press)
Böhringer, H., & Fabian, A. C. 1989, MNRAS, 215, 147
Böhringer, H., Voges, W., Fabian, A. C. Edge, A. C., & Neumann, D. 1993, MNRAS, 264, L25
Böhringer, H., Nulsen, P. E. J., Braun, R., & Fabian, A. C. 1995, MNRAS, 274, L67
Böhringer, H., Neumann, D. M., Schindler, S., & Huchra, J. P. 1997, ApJ, 482, 648
Böhringer, H. 1999, in Proceedings of the Workshop, Diffuse Thermal and Relativistic Plasma in Galaxy Clusters, April 19–23, 1999, ed. H. Böhringer, L. Feretti, & P. Schuecker (Ringberg Castle), MPE Report 271, 115
Böhringer, H., Belsole, E., Kennea, J., et al. 2001, A&A, 365, L181
Bondi, H. 1952, MNRAS, 112, 195
Braine, J., Wyrowski, F., Radford, S. J. E., Henkel, C., & Lesch, H. 1995, A&A, 293, 315
Buote, D. A., & Canizares, C. R. 1994, ApJ, 427, 96
Buote, D. A., & Canizares, C. R. 1996, ApJ, 457, 177
Burns, J. O. 1990, AJ, 99, 14
Burns, J. O., Sulkanen, M. E., Gisler, G. R., & Perley, R. A. 1992, ApJ, 388, L49
Canizares, C. R., Clark, G. W., Markert, T. H., et al. 1979, ApJ, 234, L33
Canizares, C. R., Clark, G. W., Jernigan, J. G., & Markert, T. H. 1982, ApJ, 262, L32
Cardiel, N., Gorgas, J., & Aragon-Salamanca, A. 1998, MNRAS, 298, 977
Cohen, J. G., & Ryzhov, A. 1997, ApJ, 486, 230
Cowie, L. L., & Binney, J. 1977, ApJ, 215, 723
Cowie, L. L., Hu, E. M., Jenkins, E. B., & York, D. G. 1983, ApJ, 272, 29
Churazov, E., Forman, W., Jones, C., & Böhringer, H. 2000, A&A, 356, 788
Churazov, E., Brüggen, M., Kaiser, C. R., Böhringer, H., & Forman, W. 2001, ApJ, 554, 261
Churazov, E., Sunyaev, R., Forman, W., & Böhringer, H. 2001, MNRAS, submitted
Crawford, C. S., & Fabian, A. C. 1992, MNRAS, 259, 265
Crawford, C. S., Allen, S. W., Eebeling, H., Edge, A. C., & Fabian, A. C. 1999, MNRAS, 306, 857
den Herder, J. W., Brinkman, A. C., Kahn, S. M., et al. 2001, A&A, 365, L7
Dreher, J. W., Carilli, C. L., & Perley, R. A. 1987, ApJ, 316, 611
Edge, A. C., Ivison, R. J., Smail, I. R., Blain, A. W., & Kneib, J.-P. 1999, MNRAS, 306, 599
Edge, A. C. 2001, MNRAS, 328, 762
Efstathiou, G., Frenk, C. S., White, S. D. M., & Davis, M. 1988, MNRAS, 235, 715
Fabian, A. C., & Nulsen, P. E. J. 1977, MNRAS, 180, 479
Fabian, A. C., Nulsen, P. E. J., & Canizares, C. R. 1984, Nature, 310, 733
Fabian, A. C. 1994, ARA&A, 32, 277
Fabian, A. C., Canizares, C. R., & Böhringer, H. 1994, ApJ, 425, 40
Fabian, A. C. 1999, in Diffuse Thermal and Relativistic Plasma in Galaxy Clusters, ed. H. Böhringer, L. Feretti, & P. Schuecker, MPE Report 271, p. 123
Fabian, A. C., Sanders, J. S., Ettori, S., et al. 2000, MNRAS, 318, 65

Fabian, A. C., Mushotzky, R. F., Nulsen, P. E. J., & Peterson, J. R. 2001a, MNRAS, 321, 20
Fabian, A. C., Sanders, J. S., Ettori, S., et al. 2001b, MNRAS, 321, L33
Ford, H. C., Holland, C., Harms, R. J., et al. 1994, ApJ, 435, L27
Feretti, L., Dallacasa, D., Govoni, F., et al. 1999, A&A, 344, 472
Franx, M., Illingworth, G., & Heckman, T. 1989, ApJ, 344, 613
Garasi, C., Loken, C., Burns, J. O., & Roettiger, K. 1998, MNRAS, 298, 697
Ge, J. P., & Owen, F. N. 1993, AJ, 105, 778
Heckman, T. M., Illingworth, G. D., Miley, G. K., & van Breugel, W. J. M. 1985, ApJ, 299, 41
Heckman, T. M., Baum, S. A., van Breugel, W. J. M., & McCarthy, P. 1989, ApJ, 338, 48
Ikebe, Y., Makishima, K., Ezawa, H., et al. 1997, ApJ, 481, 660
Ikebe, Y., Makishima, K., Fukazawa, Y., et al. 1999, ApJ, 525, 58
Jansen, F., Lumb, D., Altieri, B., et al. 2001, A&A, 365, L1
Johnstone, R. M., Fabian, A. C., Edge, A. C., & Thomas, P. A. 1992, MNRAS, 255, 431
Kassim, N., Perley, R. A., Erickson, W. C., & Dwarakanath, K. S. 1993, AJ, 106, 2218
Kaastra, J. S., Ferrigno, C., Tamura, T., et al. 2001, A&A, 365, L99
Kley, W., & Mathews, W. G. 1995, ApJ, 438, 107
Macchetto, F., Marconi, A., Axon, D. J., et al. 1997, ApJ, 489, 579
Makishima, K., Ezawa, H., Fukazawa, Y., et al. 2001, PASJ, 53, 401
Markevitch, M., Ponman, T. J., Nulsen, P. E. J., et al. 2000, ApJ, 541, 542
Mathews, W. G., & Bregman, J. N. 1978, 224, 308
Matsushita, K., Belsole, E., Finoguenov, A., & Böhringer, H. 2001, A&A, submitted
Mazzotta, P., Markevitch, M., Vikhlinin, A., et al. 2001, MNRAS, 555, 205
McNamara, B. 1997, in Galactic and Cluster Cooling Flows, ed. N. Soker, PASP (San Francisco), 109
McNamara, B. 2000, in Constructing the Universe with Clusters of Galaxies, IAP Symp., Paris July 2000 [astro-ph/0012331]
McNamara, B., & O'Connell, R. W. 1989, AJ, 98, 2018
McNamara, B., & O'Connell, R. W. 1993, AJ, 105, 417
McNamara, B., Wise, M., Nulsen, P. E. J., et al. 2000, ApJ, 534, L135
Molendi, S., & Pizzolato, F. 2001, ApJ, in press [astro-ph/0106552]
Molendi, S., & Gastaldello, F. 2001, A&A, in press [astro-ph/0106553]
Mould, J. R., Oke, J. B., DeZeeuw, Nemec, J. M. 1990, AJ, 99, 1823
Mushotzky, R. F., & Szymkowiak, A. E. 1988, in Cooliong Flows in Clusters of Galaxies, ed. A. C. Fabian (Kluwer Acad. Publ.), Math. and Phys. Sciences Ser., 229, 53
Nulsen, P. E. J. 1986, MNRAS, 221, 377
O'Dea, C. P., Baum, S. A., Maloney, P. R., Taccone, L. J., Sparks, W. B. 1994, ApJ, 422, 467
Owen, F. N., Eilek, J. A., Keel, W. C. 1990, ApJ, 362, 449
Owen, F. N., & Eilek, J. A. 1998, ApJ, 493, 73
Owen, F. N., Eilek, J. A., Kassim, N. E. 2000, ApJ, 543, 611
Pedlar, A., Ghataure, H. S., Davies, R. D., et al. 1990, MNRAS, 246, 477
Peres, C. B., Fabian, A. C., Edge, A. C., et al. 1998, MNRAS, 298, 416
Peterson, J. R., Paerels, F. B. S., Kaastra, J. S., et al. 2001, A&A, 365, L104
Prestwich, A. H., Guimond, S. J., Luginbuhl, C. B., Joy, M. 1995, ApJ, 438, L71
Quilis, V., Bower, R. G., Balogh, M. L. 2001, MNRAS, submitted [astro-ph/0109022]
Rizza, E., Loken, C., Blinton, M., Roettiger, K., Burns, J. O., Owen, F. N. 2000, AJ, 119, 21
Rottmann, H., Mack, K.-H., Klein, U., Wielebinski, R. 1996, A&A, 309, L9
Schmidt, R. W., Allen, S. W., Fabian, A. C. 2001, MNRAS, in press [astro-ph/0107311]
Schmidt, R. W., & Fabian, A. C., 2001, Results presented at the conference, Tracing Evolution with Galaxy Clusters held at Sesto Pusteria, Italy, July 3rd to 6th, 2001
Schwarz, R. A., Edge, A. C., Voges, W., et al. 1992, A&A, 256, L11
Sembach, K. L., & Tonry, J. L. 1996, AJ, 112, 797
Silk, J. 1976, ApJ, 208, 646
Soker, N., & Sarazin, C. L. 1990, ApJ, 348, 73
Soker, N., White III, R. E., David, L. P., & McNamara, B. 2001, ApJ, 549, 832
Stewart, G. C., Canizares, C. R., Fabian, A. C., & Nulsen, P. E. J. 1984, ApJ, 278, 536
Strüder, L., Briel, U. G., Dennerl, K., et al. 2001, A&A, 365, L18
Tabor, G., & Binney, J. 1993, MNRAS, 263, 323
Tamura, T., Kaastra, J. S., Peterson, J. R., et al. 2001, A&A, 365, L87
Taylor, G. B., & Perley, R. A. 1993, ApJ, 416, 554
Taylor, G. B., Barton, E. J., & Ge, J.-P. 1994, AJ, 107, 1942
Taylor, G. B., Govoni, F., Allen, S. W., & Fabian, A. C. 2001, MNRAS, 326, 2
Thomas, P. A., Fabian, A. C., & Nulsen, P. E. J. 1987, MNRAS, 228, 973
Tucker, W. H., & Rosner, R. 1983, ApJ, 267, 547
Turner, M. J. L., Abbey, A., Arnaud, M., et al. 2001, A&A, 365, L27
Vikhlinin, A., Markevitch, M., & Murray, S. S. 2000, ApJ, 549, 47
Voit, G. M., & Donahue, M. 1995, ApJ, 452, 164
White, D. A., Fabian, A. C., Johnstone, R. M., Mushotzky, R. F., & Arnaud, K. A. 1991, MNRAS, 252, 72
White, S. D. M. 1996, in Les Houches Session LX, August 1993, Cosmology and large-scale structure, ed. R. Schaeffer, J. Silk, M. Spiro, & J. Zinn-Justin (Elsevier, Amsterdam) [astro-ph/9410043]
Wilman, R. J., Edge, A. C., Johnstone, R. M., Crawford, C. S., & Fabian, A. C. 2000, MNRAS, 318, 1232
Zhao, J.-H., Sumi, D. M., Burns, J. O., & Duric, N. 1993, ApJ, 416, 51